minerals

MDPI

Article

Probabilistic Modelling of Geologically Complex Veins of the Barberton Greenstone Complex at Fairview Mine, South Africa

Tyson Mutobvu [1], Hendrik Pretorius [1], Charles Johannes Muller [2] and Mahlomola Isaac Mabala [3,*]

[1] Pan African Resources, Johannesburg 2196, South Africa; hpretorius@paf.co.za (H.P.)
[2] Protek Consulting, Krugersdorp 1739, South Africa; charles@protekconsult.co.za
[3] School of Mining Engineering, University of the Witwatersrand, Johannesburg 2001, South Africa
* Correspondence: mahlomola.mabala@wits.ac.za

Abstract: Achieving accurate estimations of recoverable tonnage relies on a robust geological modelling process. To ensure this accuracy, it is crucial to incorporate information from exploration, grade control, and sampling, considering well-identified mineralization controls. However, modelling the geology of complex orebodies, especially veins, poses challenges due to their intricate mineral accumulation processes and variable structural complexities. Fairview Mine's Main Reef Complex (MRC) reef is highly discontinuous, with most of the valuable mineralized zone concentrated within localized ore shoots that intersect various lithologies, exemplifying these challenges. This study aimed to improve the modelling of veins at the mine, striving for a more accurate representation of the mineralization zones. To achieve this, a hybrid approach was employed, combining a deterministic method based on minimum curvature interpolation with a probabilistic method using anisotropic inverse distance weighting for categorical/discrete variables. The subsequent tonnage estimates showed a robust correlation with actual production output. The initial deterministic model established the large-scale geological trend, providing a foundation for estimating a probabilistic model. The iterative nature of probabilistic modelling allowed for the analysis of various probable options, facilitating the selection of the model that best captured the underlying geology. This approach enabled robust mathematical modelling while incorporating valuable input from geological knowledge and expectations.

Keywords: vein modelling; anisotropic inverse distance weighting; probabilistic modelling; minimum curvature interpolation; Barberton; geological modelling; complex geology

Citation: Mutobvu, T.; Pretorius, H.; Muller, C.J.; Mabala, M.I. Probabilistic Modelling of Geologically Complex Veins of the Barberton Greenstone Complex at Fairview Mine, South Africa. *Minerals* **2024**, *14*, 343. https://doi.org/10.3390/min14040343

Academic Editors: Nasser Madani, Mohammad Maleki, Nadia Mery and Emmanouil Varouchakis

Received: 11 December 2023
Revised: 20 March 2024
Accepted: 21 March 2024
Published: 26 March 2024

1. Introduction

Accurate estimations of recoverable tonnage depend on robust geological modelling. This accuracy can be achieved through resource modelling that thoroughly considers the constraints imposed by well-identified mineralization controls [1–6] through the use of information from exploration, grade control, and sampling. However, the geology of complex orebodies, particularly veins, is generally difficult to model due to their complicated mineral accumulation processes and associated variable structural complexities [7,8] A vein is a mineral-filled fissure or fracture in the host lithologies which was filled by mineral assemblages controlled by the fluid composition either leached from the country rocks or transported from elsewhere. These veins typically occur as tabular units and dip at a particular angle from the horizontal [9] relative to the lithological layering. Typical geometrical variations in dip, strike, and width of veins necessitate a meticulous definition of the overall vein structure during modelling. Additionally, veins often exhibit complexities such as intersections, branching, splitting, or braiding, requiring a thorough understanding of mineral enrichment along these variations for a reliable estimation of recoverable tonnage and in situ grades. Furthermore, ore formation within veins can be confined within the vein itself or extend into wall-rock alteration zones, or both, thereby complicating the delineation of the orebody. The complexity of veins is further compounded by features such as

post-mineralization faulting, folding, igneous intrusions, metamorphism, and weathering. All these factors need to be considered during the geological modelling process, making it inherently challenging and not straightforward. Grade continuity within veins is also generally limited due to the localization of high grades in ore shoots which are surrounded by barren rocks or low-grade areas. Complex, localized, erratic high grades ("nuggets") are common and affect the overall confidence in the classification of a Mineral Resource. The multi-phase style of mineral accumulation associated with veins further contributes to complex grade distributions [9–11].

Understanding vein geology and estimating grades in these formations involves using different approaches. Best practices for sampling methods specific to these deposits are discussed by [2,9–17]. Several articles such as [18–25] provide insights into handling samples from different support, which is a phenomenon commonly associated with the sampling of lode-type deposits. Effectively managing grade control and mapping is crucial when dealing with vein geology, some suggested approaches are detailed in [26–28]. The following publications highlight solutions to challenges posed by the high nuggety nature of these types of deposits [2,14,29–31]. The complexity of veins makes it difficult to accurately predict their geometry and grade continuity. As a result, it is crucial to quantify the uncertainties associated with these predictions to prevent discrepancies in tonnages and grades. This uncertainty quantification plays a crucial role in gaining a deeper understanding of the financial uncertainties involved in mining operations. Many research papers have highlighted the importance of quantifying geological and grade uncertainty and suggested different methods to address this challenge, some notable references include [31–37].

Vein system modelling can be approached either deterministically or probabilistically, employing explicit and/or implicit modelling techniques. In deterministic models, geological predictions are made at specific locations, whereas probabilistic models provide the likelihood of a geological variable at every position. When dealing with complex deposits, ref [4] suggests employing hybrid geological models that combine both deterministic and probabilistic approaches. Deterministic models handle large-scale geological controls and constrain the model's extent, while probabilistic models assess the uncertainty of geological attributes at each location. Explicit modelling, commonly referred to as wireframing, involves creating 2D sections which are later linked to create a 3D geological model. Implicit models, on the other hand, rely on mathematical functions to automatically produce geological models. Numerous case studies on vein geology modelling have been published, encompassing various techniques such as polygon method [7], wireframing [3,19], inverse distance weighting (IDW) [5], indicator kriging (IK) [5,7], multiple indicator kriging [4], 2D vertical longitudinal projection [38] radial basis function [39], sequential indicator simulation [40], direct sequential simulation [23], conditional probability [31] distance function [41], minimum curvature interpolation (MCI) [42], co-kriging [43] and total least squares [44]. For ore grade interpolation within veins, ordinary kriging (OK) [22,38,42,45] and IDW [19,46,47] are the most applied methods. However, certain case studies showcase the use of alternative methods such as nearest neighbour, lognormal kriging [48], indicator kriging [19,48], disjunctive kriging [25], sequential, Gaussian simulation [40], probability field simulation [24], artificial neural networks [49], and support vector machines [50]. Key considerations in predicting grades in veins include deciding whether to estimate them directly or through accumulation and addressing issues related to extreme values [9].

The existing orebody at Fairview Mine presents common challenges associated with vein modelling, notably the intricate geology marked by a highly discontinuous orebody. Much of the valuable mineralized zone is concentrated within localized ore shoots that intersect various lithologies. Additional challenges involve the imperative to standardize the geological database and enhance the current grade estimation methodology to ensure accurate and reproducible tonnage estimations. Despite these challenges, the wealth of information from approximately 130 years of historical mining activities and the associ-

ated comprehensive geological mapping offers ample geological knowledge for seamless integration into geological models.

The objective of this study was to enhance the modelling of veins at the mine, striving for a more accurate representation of the mineralization zones of interest. To attain this objective, a hybrid approach that combined both deterministic and probabilistic methods, guided by the integration of geological understanding within the modelling process, was implemented. Following the delineation of mineralized zones, grade interpolation within them was conducted. Additionally, the research sought to contribute to the existing gap in knowledge regarding the modelling of veins in the Barberton Greenstone Belt (BGB), South Africa.

2. Geological Setting

The Fairview Mine, which forms part of Barberton Mines Limited, a subsidiary of Pan African Resources, is located about 45 km south of Mbombela within the BGB in South Africa. The BGB is part of the oldest nucleus of the Kaapvaal Craton, consisting of 3.55–3.2 Ga volcano-sedimentary sequence, surrounded by various generations of granodiorite gneisses and potassic granites ranging from 3.5–3.1 Ga. The greenstone belt sequence consists of the Onverwacht, Fig Tree, and Modies Groups. The Onverwacht Group is dominated by ultramafic and mafic volcanic rocks; the Fig Tree Group is composed of greywackes, shales, and cherts whilst the overlying Moodies Group is characterized by coarse-grained clastic sedimentary rocks, mainly including sandstones and conglomerates as shown in Figure 1 [51].

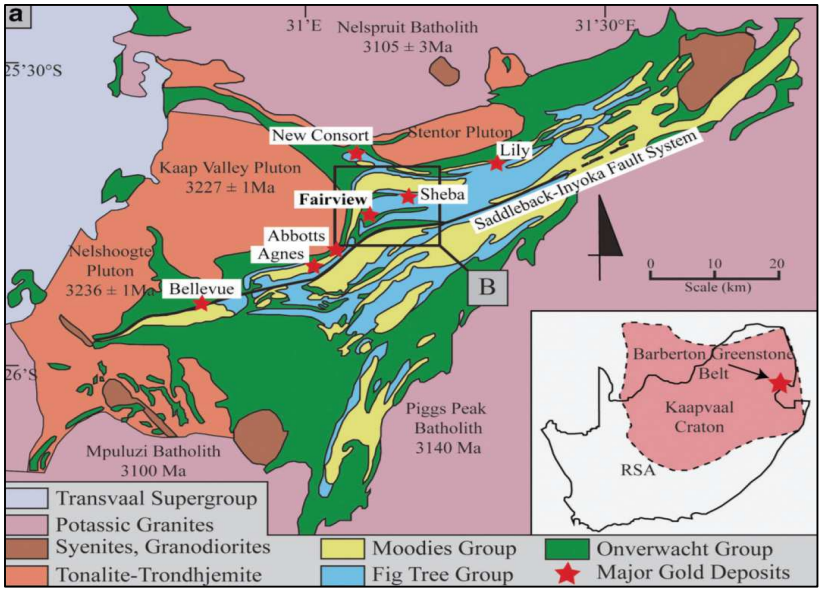

Figure 1. Regional geological map of the BGB, showing surrounding gold mines. B shows the locality of the Fairview mine in relation to other mines in the vicinity [52].

The rocks underlying the Fairview Mine area straddle the contact between the arenites of the Moodies Group to the north (Eureka Syncline) and the Fig Tree Group's greywacke and shale to the south (Ulundi Syncline). The contact is marked by the presence of the regionally identifiable Sheba Fault as shown in Figure 2. The immense force experienced during deformation has led to the refolding of the two synclines, forming steeply dipping back-to-back isoclines to the south. Within the greywacke of the Fig Tree Group, there are tight isoclinal anticlines related to thrust faults, consisting of Onverwacht Group schist (Zwartkoppie Formation) [53].

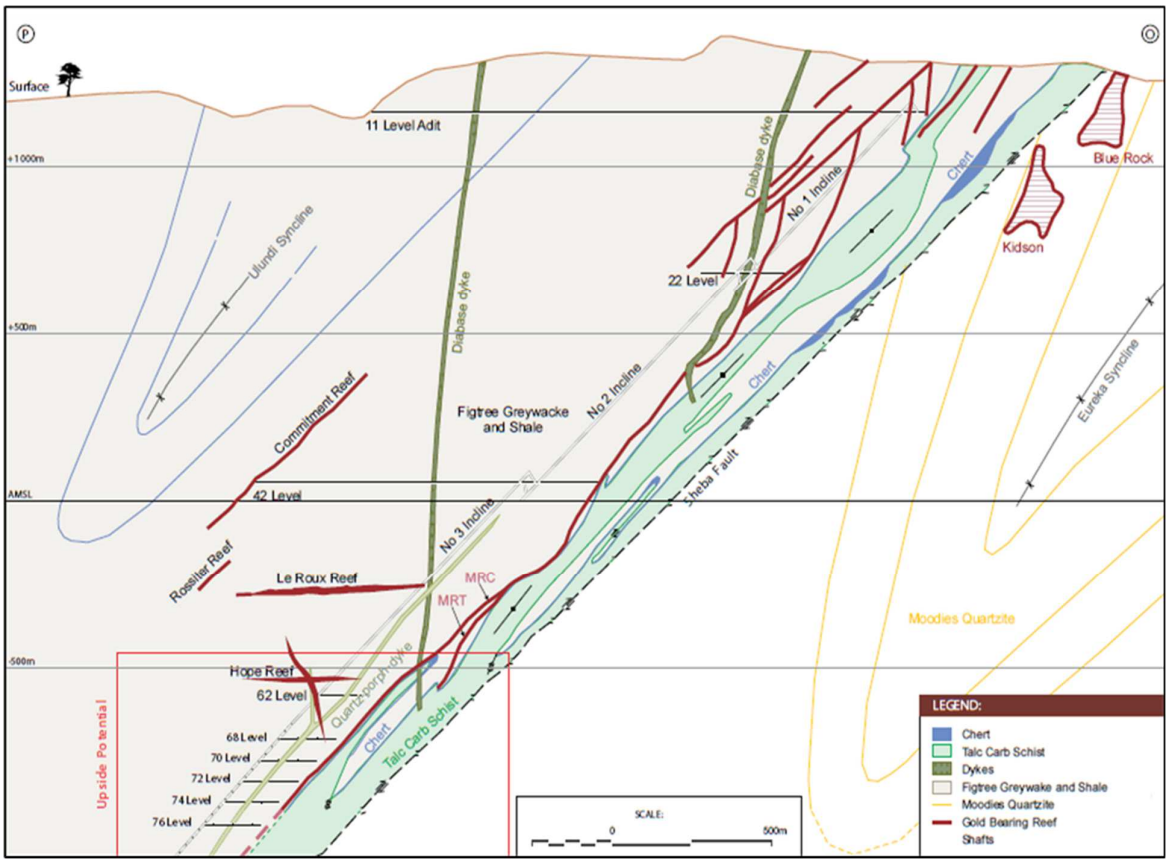

Figure 2. Local geology at the Fairview Mine, showing the MRC and the synclines associated with the Sheba fault.

The orebody at the Fairview Mine is characterized as an epigenetic hydrothermal lode gold deposit. The primary source of mineralization, where much of the ore is extracted, is the laterally extensive Main Reef Complex (MRC), as depicted in Figure 2. The MRC reef consists of refractory sulphidic ore, with its mineralization linked to an anastomosing shear system that often aligns with the stratigraphy and lithological contacts. Auriferous pyrite and arsenopyrite mineralization occur in ribbon-like shoots within the shear system and as disseminations in the surrounding wall rock. These shears are frequently defined by quartz-carbonate veining, and the host rock can undergo sericitization and carbonatization on either side of the shear [54]. High-grade gold-sulfide ore is confined to several steeply plunging linear ore shoot layers. These layers are locally thinned and thickened in both the easterly and northerly directions. Mineralization controls are not always physically visible where the deposition has occurred, and they cut across different stratigraphy from the hangingwall graywacke to the footwall greenschist. Sulfides are common throughout the gold mineralization, with pyrite and pyrrhotite. Arsenopyrite is commonly associated with quartz veining in areas of highest-grade gold mineralization [52]

3. Methodology

The geological modelling of significant mineralized zones, or ore shoots, and the subsequent estimation of grades primarily relied on data from in-stope chip samples and underground exploration drill holes. The vein modelling process involved two main steps:

1. The initial step employed a deterministic implicit approach based on the MCI to model the overall, large-scale trend of mineralization. This approach generated a simplified solid representation outlining the general shape and boundaries of the ore body, referred to as the ore envelope.

2. Following this, a probabilistic approach was applied to model ore shoots within the ore envelope. This involved using an anisotropic inverse distance weighting technique (AIDW), resulting in the delineation of multiple mineralized zones within the deterministic solid.

Within the identified mineralized zones, the process of grade interpolation was executed using OK. Before interpolation, a series of standard procedures were adhered to, encompassing sample analysis, top cutting, variography, and kriging neighbourhood analysis (KNA). Following the interpolation, the resulting grade model underwent validation. Additionally, preliminary analyses were conducted on Selective Mining Units (SMU), and an assessment of reasonable prospects for eventual economic extraction (RPEEE) was carried out. All these processes were implemented using Datamine Studio RM version 1.10 software [54].

3.1. Sampling and Interpolation Data

Due to the historical nature of mining and exploration, most data stems from in-stope chip samples. The dataset comprises 68,854 chip samples, taken at a grid spacing of 2 m (m) × 2 m, along with data from 9 underground exploration boreholes. The chip samples and drill holes were composited to the same composite length in order to ensure the same support. Their respective mean and variance values were then calculated and compared to determine if they could be combined and used together for further analysis. Although they were found to be slightly different, the difference was within an acceptable range of 5%.

The chip sample dataset was provided in a point format and included spatial coordinates, the channel width (CW), accumulation (CMGT), stoping width (SW), gold grades (Au), and the sample length. The channel width represents the length of the mapped orebody as shown in Figure 3. An artificial 3 m waste zone (WZ) with a grade of less than 0.05 g/t (i.e., grade less than the detection limit) was introduced above and below the CW, resulting in the reef zone (RZ) between WZs. This re-coding of data was performed to confine the estimation within the RZs (representing mineralized zones) and transform the chip sample point data into a format resembling drill-hole data, as shown in Figure 3. Consequently, the CW became synonymous with the mineralized zones represented by the RZ.

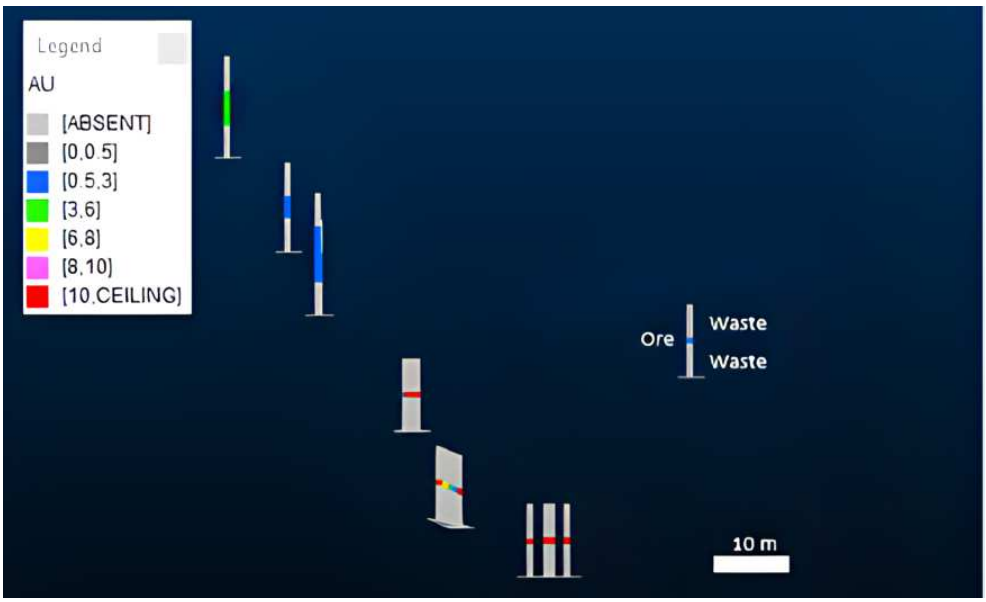

Figure 3. Reconfigured sample data.

RZ exhibits variability from sample to sample. To establish uniform sample support, the reconfigured sample data was composited to regular lengths of 0.5 m. The compositing process ensured that all samples were included in one of the composites, with adjustments made to the composite length as needed. The determination of composite length was influenced by factors such as variance, deposit characteristics, parent cell size, and mining method. Figure 4a–c displays the histograms of sample lengths of RZ samples only, lengths of RZ and WZ samples, and the resultant 0.5 m composites of the lengths of RZ and WZ samples.

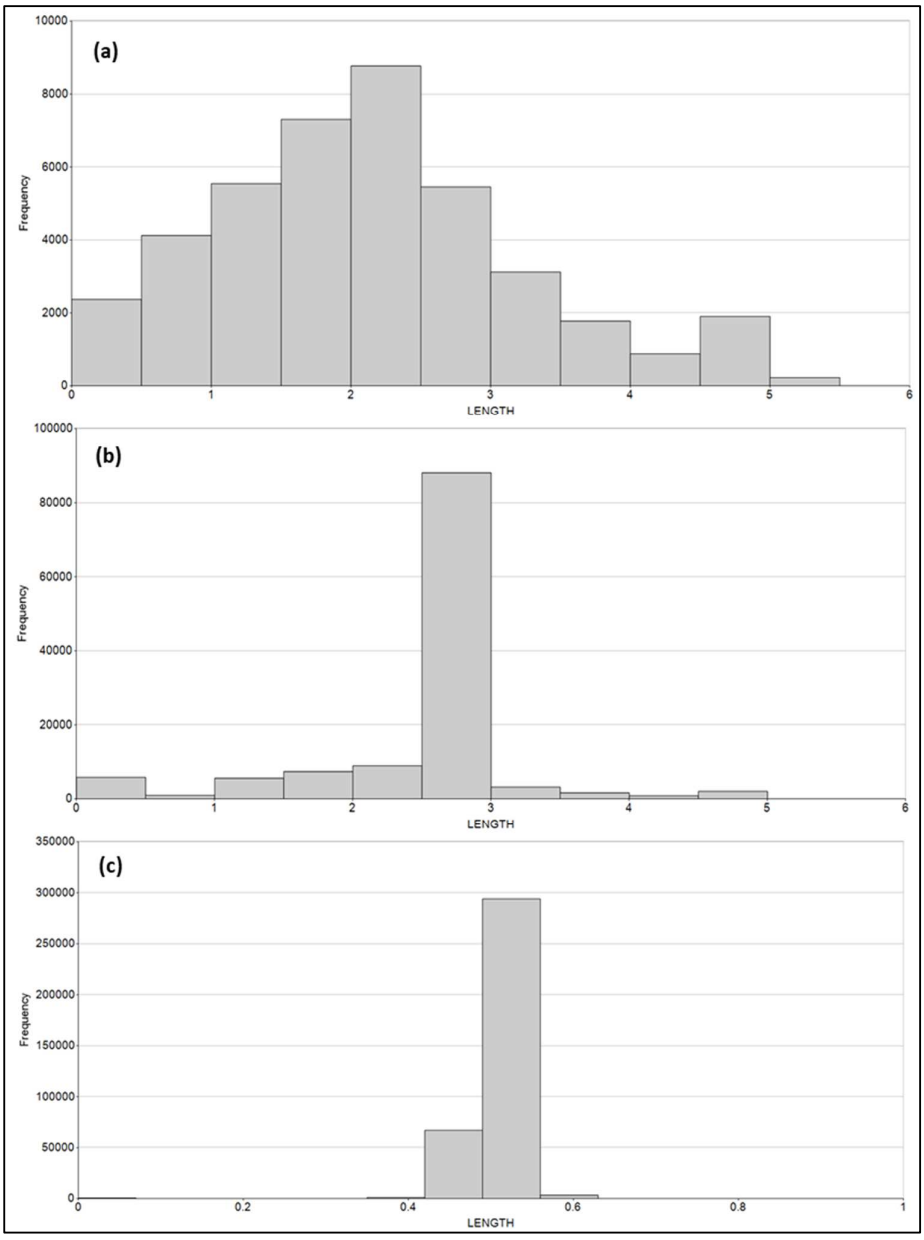

Figure 4. (**a**) Histogram of lengths of RZ samples only (in m), (**b**) Histogram of lengths of RZ and WZ samples (in m), (**c**) Histogram of 0.5 m composites of RZ and WZ samples (in m).

3.2. Deterministic Modeling

The choice of using the MCI method in Datamine Studio RM was driven by its capacity to maintain a practical level of continuity between points and generate realistic geological structures, even when dealing with intricate data inputs. This method is well-suited for a broad spectrum of input configurations, encompassing irregular hangingwall (HW) and

footwall (FW) layouts, as well as scenarios where neighbouring sample elevations exhibit significant variation [55]. This flexibility permits the consideration of a broader range of data inputs, especially in cases where the structure's trend is not inherently planar. The algorithm and underlying mathematics that form the basis of the MCI method are thoroughly documented in the literature [56–58], and will therefore not be repeated in this manuscript.

3.3. Domaining

Prior domaining had been carried out in earlier mine studies, separating the orebody into two stationary domains, i.e., domain 1 (representing the lower grade zone with an average sample grade of 3.98 g/t) and domain 2 (being the higher-grade zone with an average grade of 33.44 g/t). This domaining was established based on historical production data, identification of inflection points on cumulative probability plots, and informed geological understanding. This paper adopted the domains as delineated in previous mine studies.

3.4. Probabilistic Modelling

The AIDW technique for categorical or discrete variables was chosen to probabilistically model ore shoots for each domain within the deterministic model for several reasons. Primarily, it overcomes the issues of string and screening effects associated with kriging. Secondly, because of its simplicity in implementation, it does not necessitate a prior variogram model or solving kriging weights equations. Crucially, the most probable categorical variable at each location can be easily extracted from the interpolation results. Consideration of anisotropy allows for the incorporation of spatial continuity/discontinuity and accounts for geological variations in different directions [5,59]

The application of IDW for modelling geological contacts with categorical or discrete variables was initially proposed by [59] Subsequent refinement was introduced by [5] who integrated a search ellipsoid into the method, allowing consideration of spatial continuity and anisotropy. In this study, we adapted the anisotropic IDW method proposed by [5], this approach enables the definition of the ellipsoid's orientation for each block in the model, accommodating the local variability of ore shoot geometry and orientation.

In our study, the composited output assay data is uniquely flagged with mineralized codes (Code = 1 for mineralized zone above 0.05 g/t and Code = 2 for waste). The mineralized zone is the area with samples comprising the gold grade above the detection limit (i.e., Au $\geq$ 0.05 g/t), whilst all the material below 0.05 g/t is regarded as waste. The inverse distance to the power of two (IDW2) for categorical or discrete variables was employed as follows:

- The two categories (k), mineralized zone (k = 1) and waste (k = 2) were converted to a matrix of indicators, whereby the presence of each category at each known location u_i is given an indicator of 1 and its absence is made 0. That is:

$$\begin{aligned} i(u_i;k) &= Prob\,\{category\ k\ being\ present\ at\ location\ u_i\} \\ &= \begin{cases} 1,\ if\ category\ k\ is\ present\ at\ u_i \\ 0,\ if\ category\ k\ is\ present\ at\ u_i \end{cases} \end{aligned} \quad (1)$$

- IDW2 is then used to interpolate estimates of each category's indicators at unsampled locations based on several search and neighbourhood parameters. The distribution of uncertainty for the categories at each unsampled location is thus directly estimated. In other words, the probability distribution at any unknown location $\boldsymbol{u}$ in each domain will consist of estimated probabilities for each category (p_k^*), as described by Equations (2) and (3):

$$p_k^* = i^*(u;k) = \sum_{i=1}^{n} w_i i(u_i;k),\ k = 1,\ 2, \quad (2)$$

$$w_i = \frac{\left(\frac{1}{d_i^2}\right)}{\sum_{i=1}^{n}\left(\frac{1}{d_i^2}\right)}, \; i = 1, \ldots, n, \tag{3}$$

where w_i are IDW2 weights given to the input data and d_i are the Euclidean distances between the target location and sample points.

- Through a process of iteration, multiple realizations at different probabilities of mineralized zones were visualized and iteratively compared to the existing geological mapping, conceptual models, historic production information, and sample data. The probability level that best fitted the geologic interpretations and database was selected as optimal.

3.5. Grade Interpolation and Validation

The first step of grade interpolation was top capping, which was used to cut extremely high grades to control their influence on the estimation while taking a carefully balanced approach to retain the localized high-grade nature of the deposit. Figure 5a,b demonstrates the normal probability plots used to select the capping thresholds for domains 1 and 2, based on the visual analysis of inflection points (see intersection of red lines Figure 5a,b) in the trend of the data. The selection of the capping values was also guided by historical production data and geological expectations for each domain.

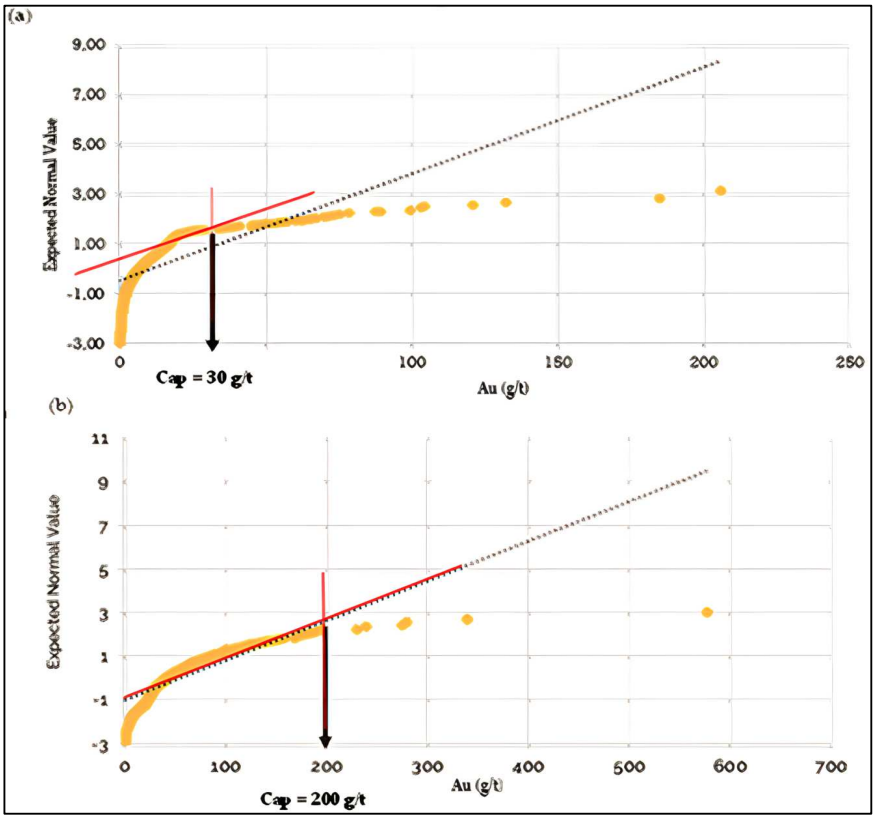

Figure 5. Normal probability plots for (**a**) domain 1 and (**b**) domain 2.

The Au grade capping set for domain 1 is 30 g/t, while domain 2 has a higher cap of 200 g/t. It is important to note that the orebody has a notably high grade, with frequent occurrences of "free gold" as evidenced by actual production data. In the case of domain 2, the decision to implement a less restrictive capping level is informed by the presence of a considerable number of very high-grade samples. Ignoring these samples could lead to a significant underestimation of grades and associated tonnages in the high-grade zones.

Instead, the potential impact of high-grade samples beyond their region of influence is rather restricted by controlling search parameters.

Three-dimensional (3D) directional variogram calculations were then performed on composite data for individual domains, with variance values normalized to a sill representing the population variance. The variograms were calculated in a rotated reference plane to follow the orientation of the principal controlling structures as shown in Figure 6. The variogram models aimed at accurately capturing the direction and extent of spatial continuity of mineralization within each specific estimation domain. Variograms with the longest range of spatial continuity were chosen for interpolation, as they indicate the primary anisotropic orientations. To provide a better understanding of the underlying spatial model, extreme values that were determined from the grade capping process were cut to remove unnecessary noise/variance during variography. The orientation of search ellipsoids was preferentially aligned with the principal controlling feature, as depicted in Figure 6.

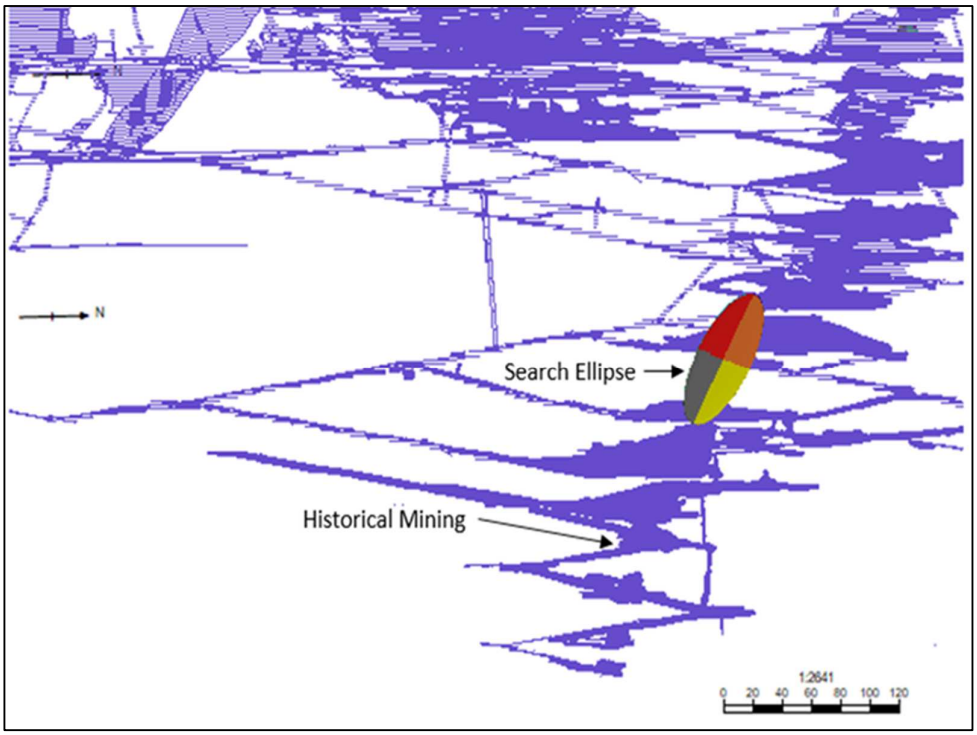

Figure 6. The search ellipse in relation to the orebody and historical mining data.

OK was employed for estimating the MRC mineralized zones per domain. Kriging, being an unbiased linear estimation technique, relies on the variance relationships of spatial samples, as indicated by the variogram. The selection of OK is driven by its widespread and proven effectiveness in grade estimation, particularly in scenarios like this study where geological controls have been distinctly defined within well-established mineralized zones. The ample availability of sample data further justifies the utilization of OK. For a more in-depth understanding of the OK method, a detailed explanation is provided in [60,61].

The grade interpolation process began by determining the estimation unit size through the KNA tool [54] in Datamine Studio RM. KNA is a process for optimizing estimation parameters by evaluating them based on kriging efficiency (KE) and the slope of regression (SLOR). Block parameters that gave the highest KE and SLOR close to 1 were selected. Consequently, block sizes of 3 m × 3 m × 1 m were chosen; the choice was also guided by the previously used SMUs, spatial distribution of the data (i.e., 2 m × 2 m), and the geometry of the mineralized zones. Utilizing three-dimensional block models to represent the volume of mineralized zones, sub-celling was applied to ensure the block model closely

approximates the wireframe model's volume. Similarly, the minimum and maximum number of samples used were selected based on the results of KNA results which gave the highest KE and SLOR close to 1. The directional ranges determined from the modelled variograms were used to constrain the search distances and directions applied to the linear estimates. The capping of extremely high-grade values was used to limit the zone of influence that the ultra-high grades have on the estimation of the surrounding areas. Dry bulk densities, informed by laboratory data, were assigned to the model, with average density values of 2.83 t/m^3 for ore and 2.73 t/m^3 for waste.

Validation of the OK grade model primarily involved visual inspection, swath plots [62] and comparison with actual production data. This entailed reviewing sections and plans to ensure proper coding of borehole intervals and block model cells. Visual checks were conducted to assess the consistency between interpolated grades and borehole composite values. Reconciliation of actual versus modelled tonnages and average grades were later compared.

For the prediction of SMU sizes, the mineable shape optimizer (MSO) tool within the Datamine Studio RM version 1.10 was employed. MSO computes the optimal size, shape, and location of stopes for an underground mine using an input block model that contains grades or values. The MSO algorithms rely on sub-celling within the block model to define the spatial location of mineralization and search for the optimal mineable shapes that fit the orebody geometry [54]. The various stope sizes were evaluated and compared to determine the most optimal SMU. Grade tonnage curves (GTCs) [63] were constructed at different cut-off grades using stopes with a minimum width of 3 m acquired from the SMU optimization process. The GTCs for in situ Mineral Resources and the more realistic extractable Resource from MSO were compared and then used to establish the RPEEE.

4. Results

4.1. Geological Modelling

4.1.1. Deterministic Model

The resultant deterministic MCI-based model is shown in Figure 7. Notably, the model's volume surpasses that of subsequent probabilistic models because it encapsulates a more large-scale regional mineralization trend, potentially encompassing un-mineable areas or mineralization of lesser economic value. While lacking in the representation of local vein geology variability, the deterministic model serves a crucial role in determining the orientation of the principal controlling feature. It is within this model that the probabilities of mineralized zones were estimated.

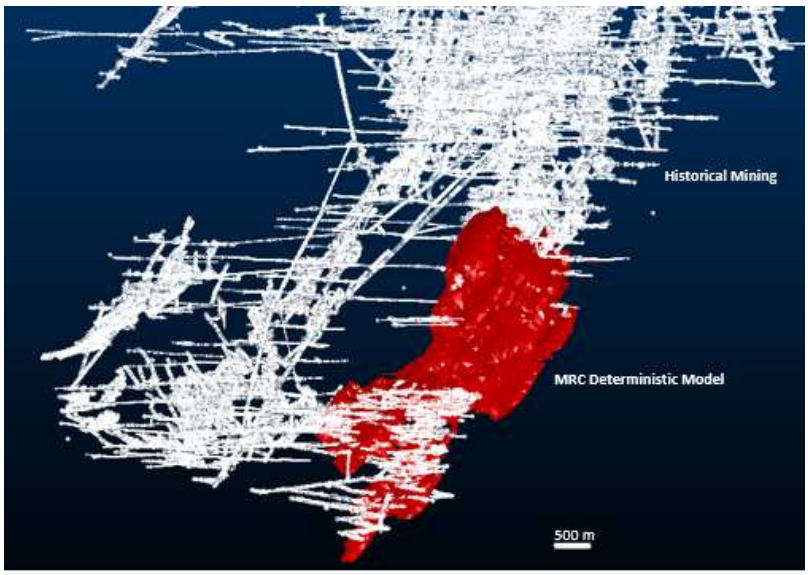

Figure 7. Deterministic model of the MRC.

4.1.2. Probabilistic Model

By using the IDW2 technique, the mineralized zones (Code = 1) probability was estimated such that the model output had values ranging between 0 and 1. Multiple models at different probabilities of mineralized zones were visualized and iteratively compared to the existing geological mapping and conceptual models. The output blocks with probabilities above 0.2 were regarded as the probable mineralized zone, as they were fitting to the geological understanding and interpretations from the known areas (i.e., sample data and historic mining This probability reflects the best fit for sample data intersections and the ratio of mineralized to non-mineralized sample volumes. Additional tools used to select the blocks are the number of samples (NS) and the block to minimum distance to the nearest (MDIS).

The final selection represented sub-domains of the geological model describing the various mineralized zones, defined by ore shoots. This probabilistic model was then employed for block modelling and subsequent grade interpolation. Figure 8 compares the full probability model and the model selected based on probability, MDIS, NS, and geological expectation.

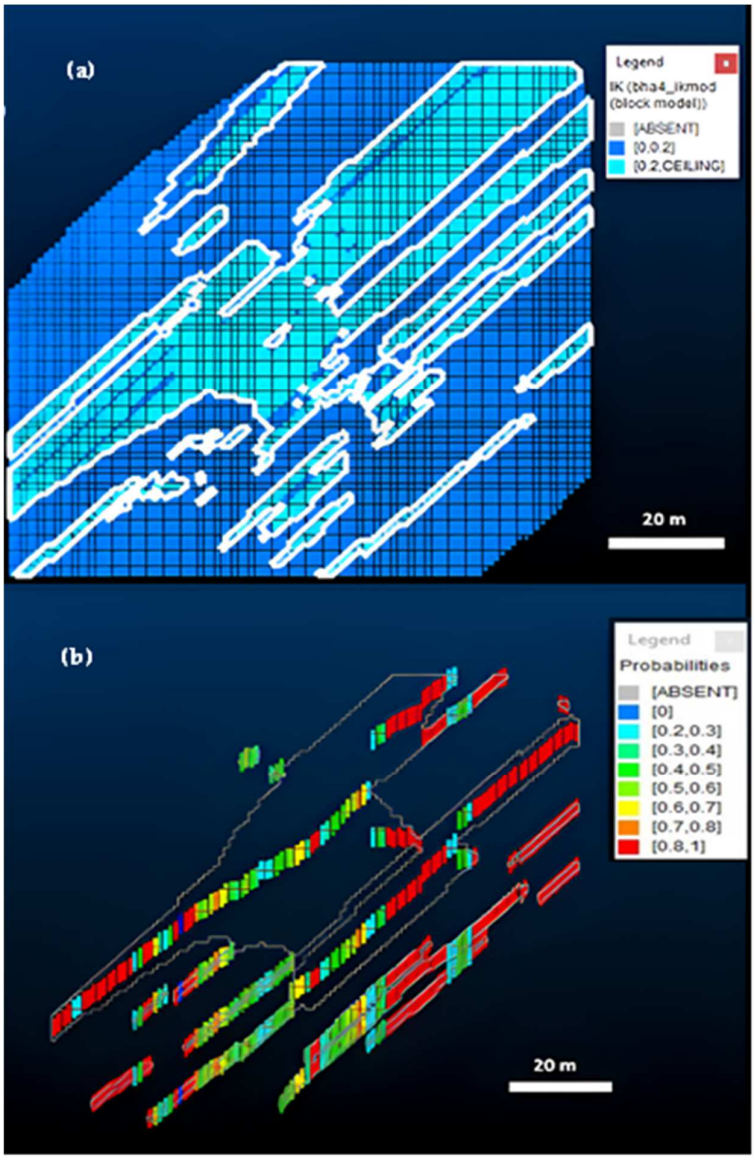

Figure 8. (**a**) Full estimated probability model and (**b**) Probability model selected based on probability = 0.2, NS, MDIS, and geological expectation.

4.2. Resource Modelling

4.2.1. Top Capping

Table 1 summarizes the grades of capped and uncapped samples in both domains 1 and 2. Although the capping has a limited effect on the sample, the main objective is to limit the effect of these extremely high grades in variography and block estimates.

Table 1. Statistics of uncapped and capped samples in domains 1 and 2.

Domain	Uncapped/ Capped	Minimum (g/t)	Maximum (g/t)	Mean (g/t)	Standard Deviation (g/t)
Domain 1	Uncapped	0	701.8	3.98	5.83
Domain 1	Capped/t	0	30.00	3.92	5.91
Domain 2	Uncapped	0	9014	33.44	53.90
Domain 2	Capped	0	200	32.88	27.40

4.2.2. Variography

The resultant 3D variogram models are depicted in Figures 9 and 10. The variograms modelled are spherical models with two nested structures with associated nugget percentages that are typical for this type of gold mineralization. These nugget effects were modelled at 46% for domain 1 and 49% for domain 2. The directional ranges determined from the variography analysis were used to guide the search distances applied during estimation.

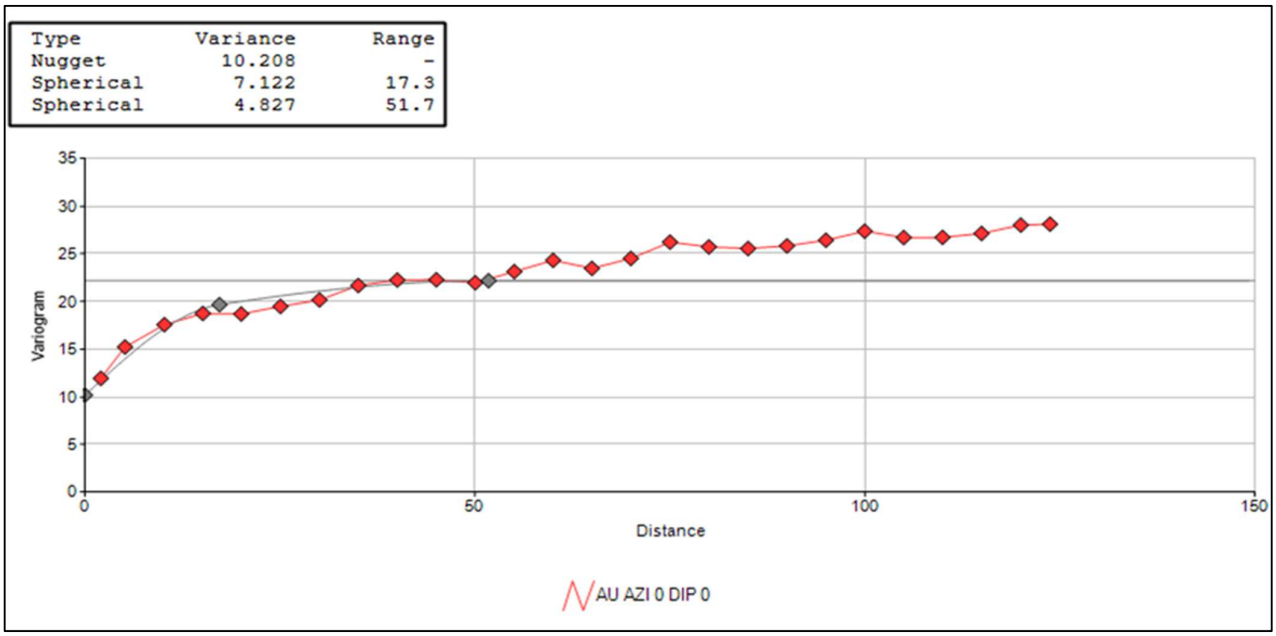

Figure 9. Variogram model for Domain 1.

4.2.3. Grade Interpolation

Table 2 summarizes the OK interpolation parameters used for each domain. Figure 11 illustrates the histogram of the total modelled grades showing an average grade of 9.21 g/t at a standard deviation of 14.76 g/t.

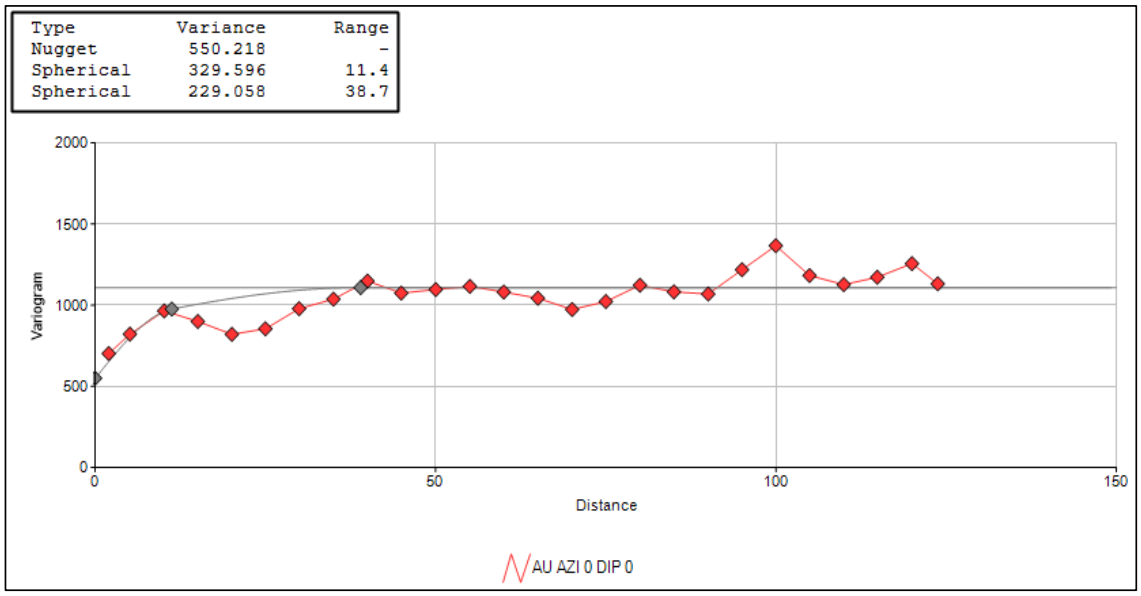

Figure 10. Variogram model for Domain 2.

Table 2. Summary of estimation parameters.

Domains	Search Distances	Rotation Search Angles (about Z, Y, X Axes)	Minimum, Maximum, Samples	Cell Sizes (X, Y, Z)	Top-Cuts
Domain 1	Linear estimate 25 m × 50 m × 5 m;	−30°, 55°, 25°	1;20	5 m × 5 m × 1 m	30 g/t Au
Domain 2	Linear estimate 25 m × 50 m ×5 m	−30°, 55°, 25°	1;20	5 m × 5 m × 1 m	200 g/t Au

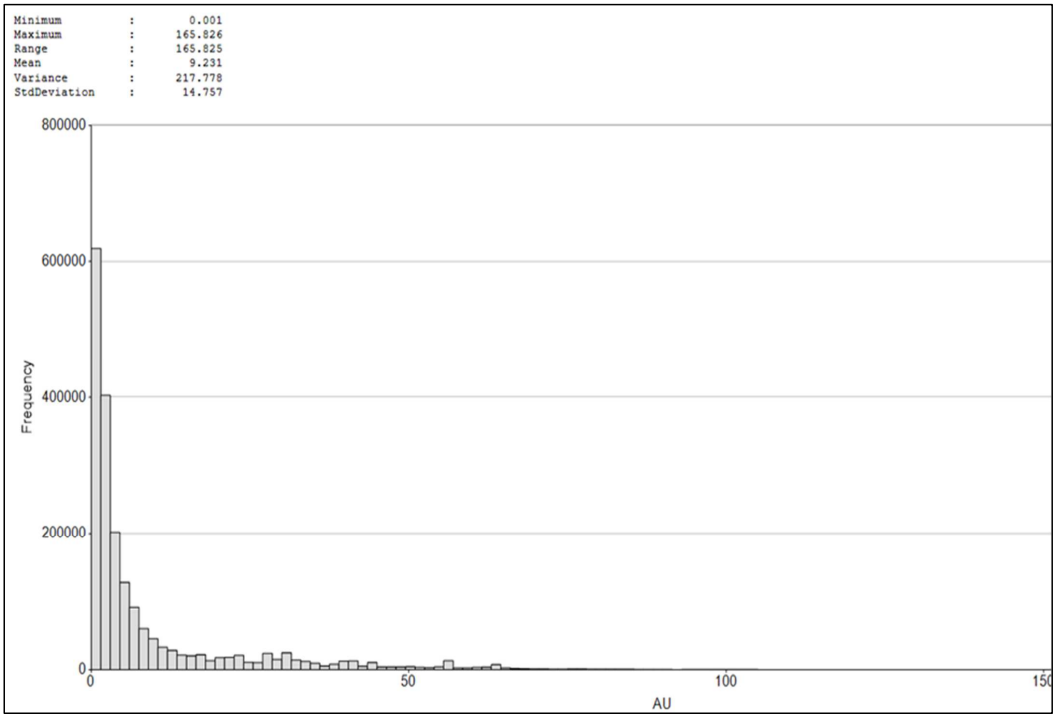

Figure 11. Histogram of estimated grades (in g/t).

4.2.4. Model Validation

Interpolated grades are examined relative to borehole composite values through visual checks, one example of the checks is demonstrated in Figure 12. The estimated blocks and data compare well in areas where sufficient data exist. Areas where discrepancies exist due to insufficient data can be targeted for future sampling or drilling.

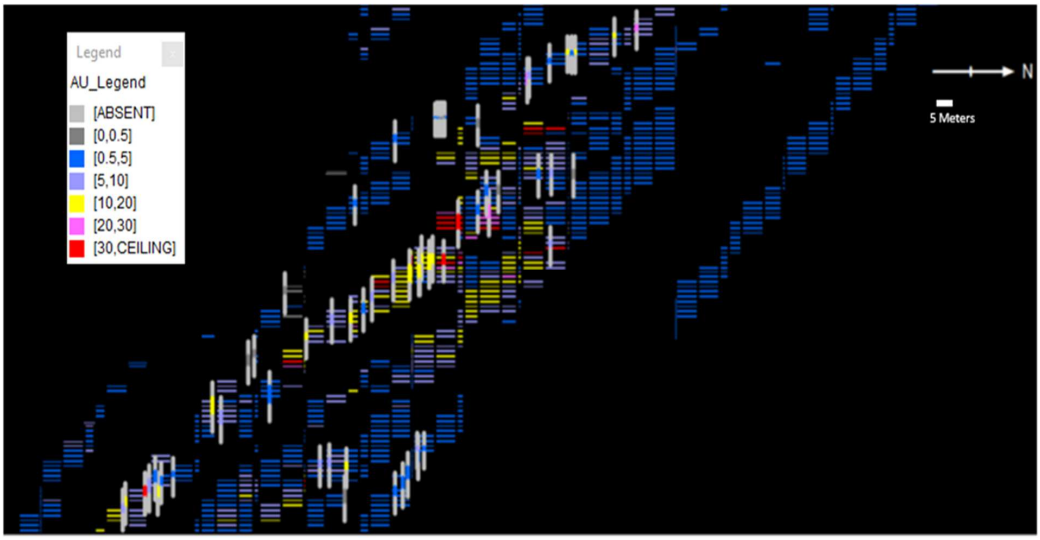

Figure 12. Model vs. the underlying data used for estimation.

The interpolated grades relative to borehole composite values were also checked through 20 m slice swath plots as shown in Figures 13–18. Although the domains are expected to be homogenous, there is still a potential for local trends considering the nature of the orebody. The values from the borehole data and block estimates indicate that the model follows the local trend within the domain and optimal block estimates exist within each slice. The model values in domain 1 are generally lower than values from the composite due to the conservative application in top capping.

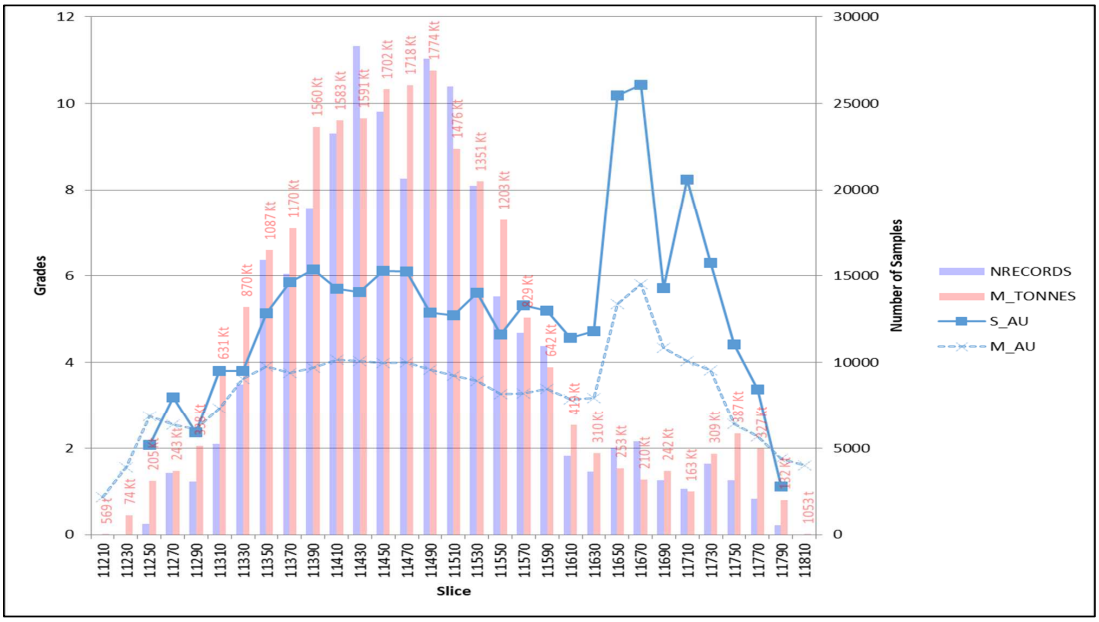

Figure 13. Domain 1 swath plots in the easting direction (NRECORDS = number of samples, M_TONNES = modelled tonnes, S_AU = average composite grade, M_AU = average estimated grade).

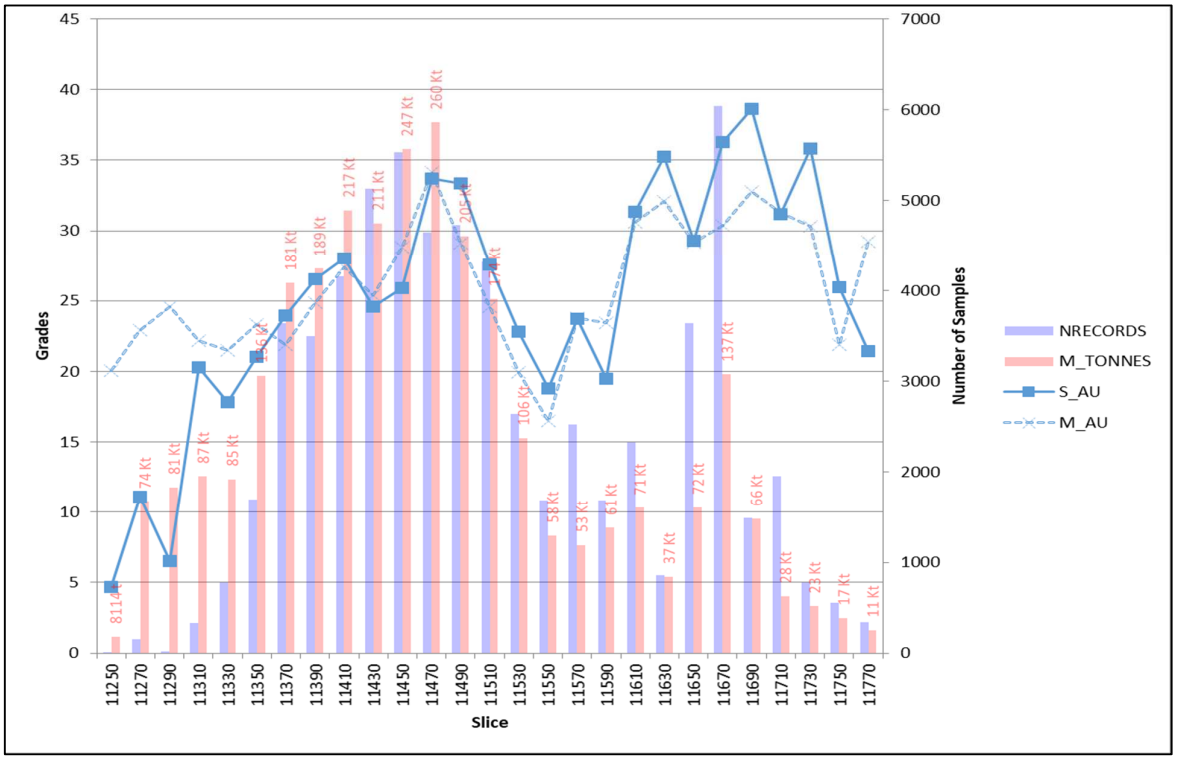

Figure 14. Domain 2 swath plots in the easting direction (NRECORDS = number of samples, M_TONNES = modelled tonnes, S_AU = average composite grade, M_AU = average estimated grade).

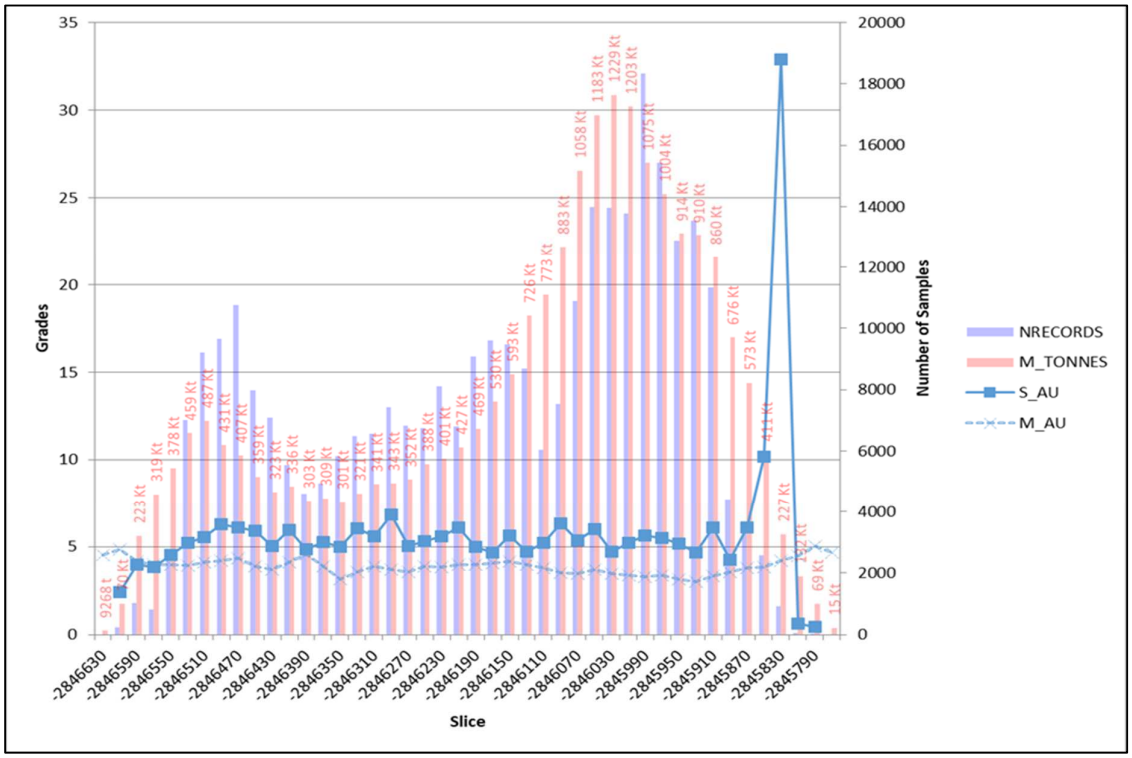

Figure 15. Domain 1 swath plots in the northing direction (NRECORDS = number of samples, M_TONNES = modelled tonnes, S_AU = average composite grade, M_AU = average estimated grade).

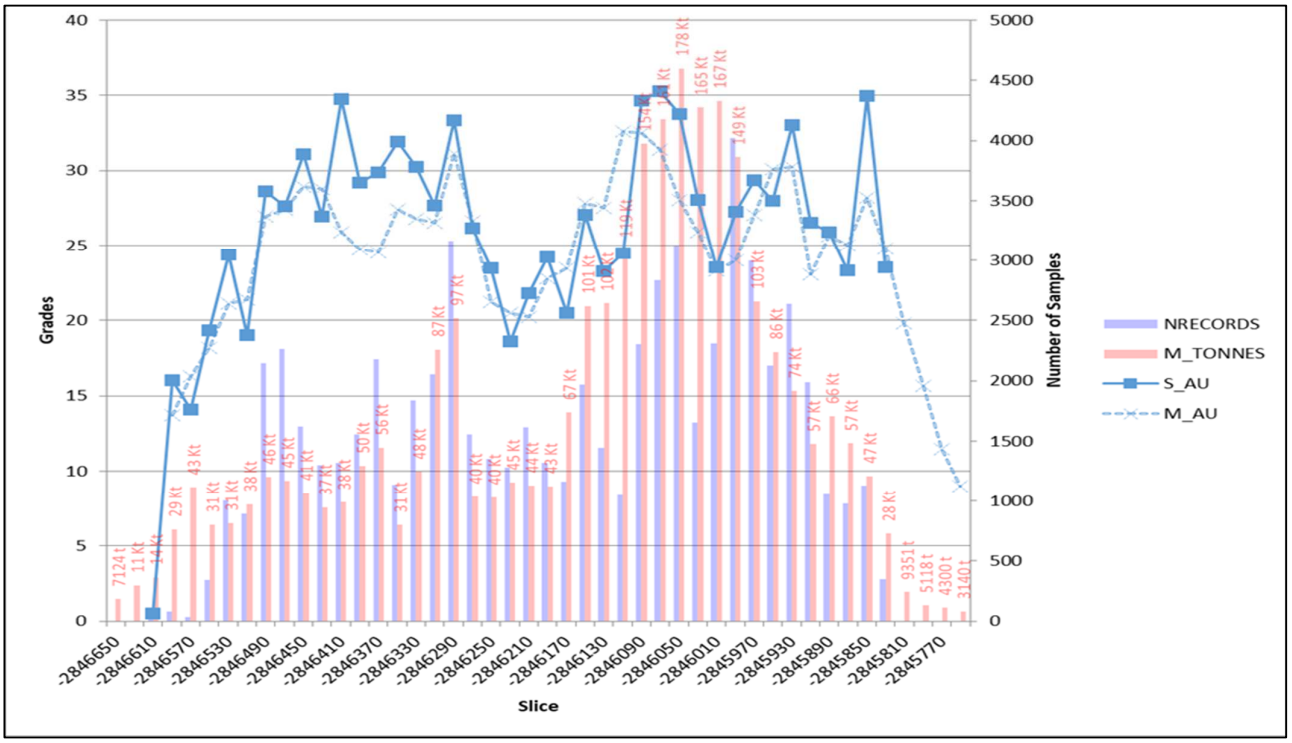

Figure 16. Domain 2 swath plots in the northing direction (NRECORDS = number of samples, M_TONNES = modelled tonnes, S_AU = average composite grade, M_AU = average estimated grade).

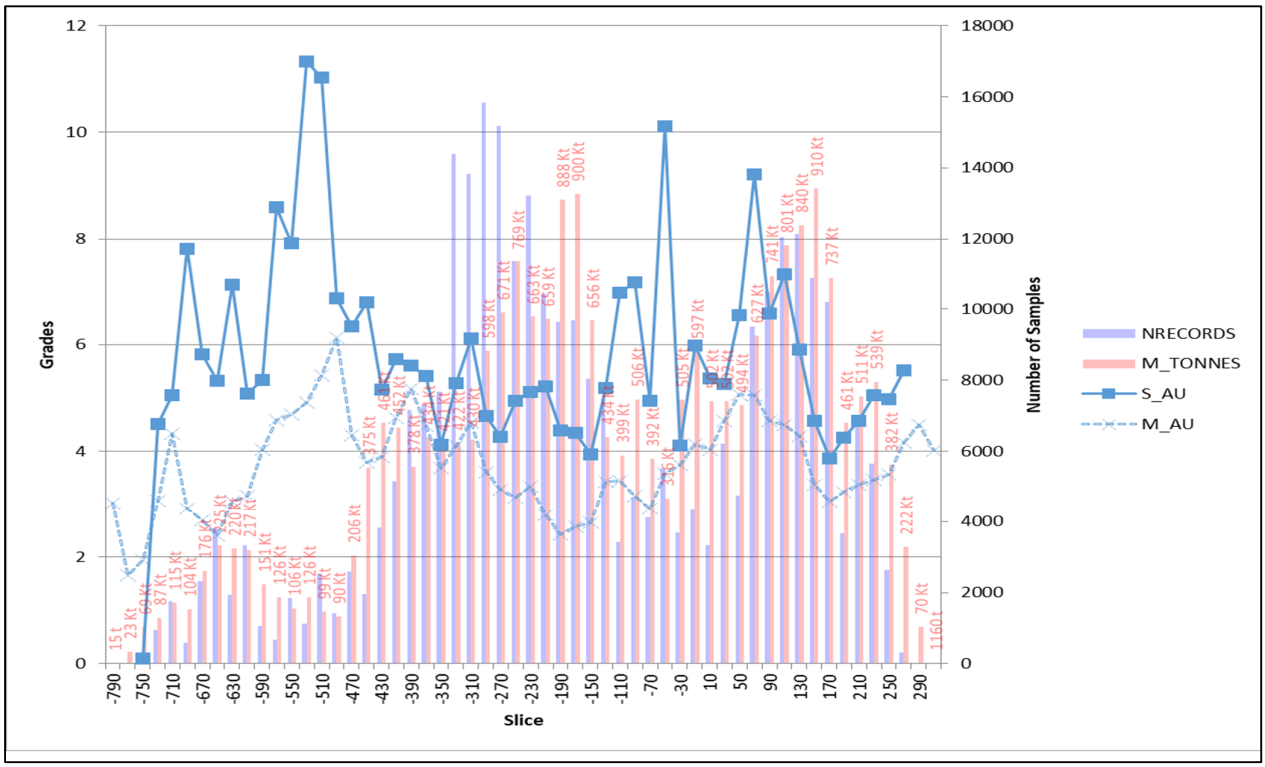

Figure 17. Domain 1 swath plots in the elevation direction (NRECORDS = number of samples, M_TONNES = modelled tonnes, S_AU = average composite grade, M_AU = average estimated grade).

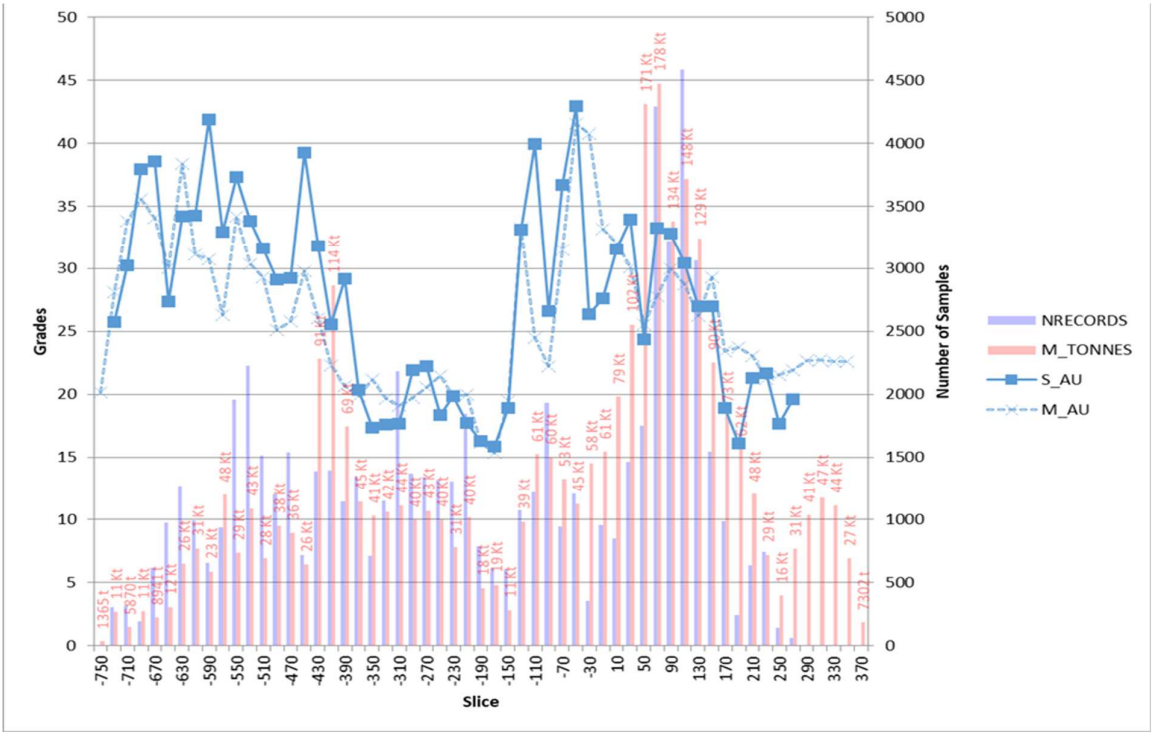

Figure 18. Domain 2 swath plots in the elevation direction (NRECORDS = number of samples, M_TONNES = modelled tonnes, S_AU = average composite grade, M_AU = average estimated grade).

The reconciliation data in Table 3, comparing actual and estimated tonnages and average grades from the three primary stoping areas, indicates that the geological modelling approach generally aligned with expected tonnages. Nevertheless, there were discrepancies: the average grade in Stope 1 was underestimated, while the mean grade was overestimated in Stope 3. The variance between actual and estimated grades can likely be attributed to the model incorporating the latest samples. It is anticipated that this discrepancy will be adequately addressed in the subsequent reconciliation analysis, as the model continues to incorporate more up-to-date information.

Table 3. Reconciliation of actual versus modelled tonnages and average grades.

Workplace	Actual		Modelled (Including Waste)		Variance	
	Tonnes (t)	Au (g/t)	Tonnes (t)	AU (g/t)	Tonnes (%)	Au (%)
Stope 1	317	11.11	308	9.82	−3%	−12%
Stope 2	2918	27.82	2898	26.60	−1%	−4%
Stope 3	116	22	119	29.31	3%	33%

4.2.5. Reasonable Prospect for Eventual Economic Extraction

MSO analysis showed a 15 m × 15 m block to be less optimal in terms of grade, whilst a 25 m × 25 m SMU brings additional waste into the ore stream. Based on the interpolated grade model, 3 m × 3 m to 6 m × 6 m were found to be the optimal SMU sizes for Mineral Resource reporting as shown in Figure 19. Further assessment considering other factors such as engineering (including geotechnical, mining, and processing parameters), metallurgical, legal, infrastructural, and economic assumptions are applied by the mine planning engineer. The reasonable prospects for eventual economic extraction have been demonstrated through the application of an appropriate level of consideration of the

potential viability of Mineral Resources MSO. In the case of Mineral Resource reporting, the SMU must match the design SMU chosen by the Mine Planning Engineer.

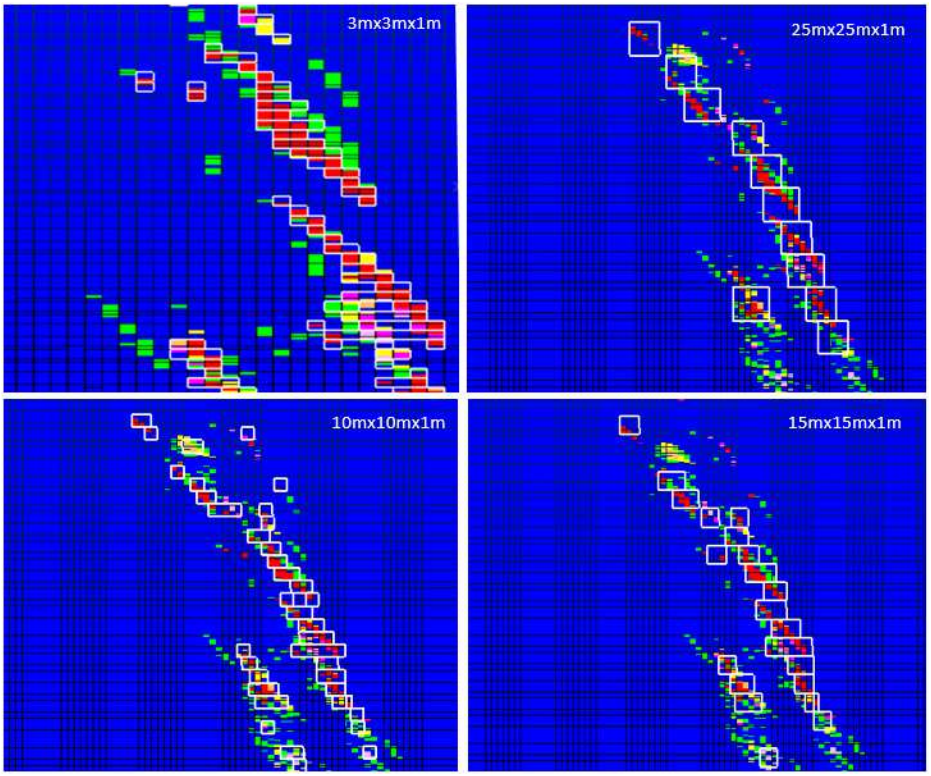

Figure 19. A section of MSO designs from 3 × 3 m to 25 × 25 m.

The GTC was adjusted to account for several modifying factors to approximate or estimate the potentially mineable material available at various cut-off grades. Figure 20 shows the GTC for in situ Mineral Resources compared with more realistic Resources from MSO.

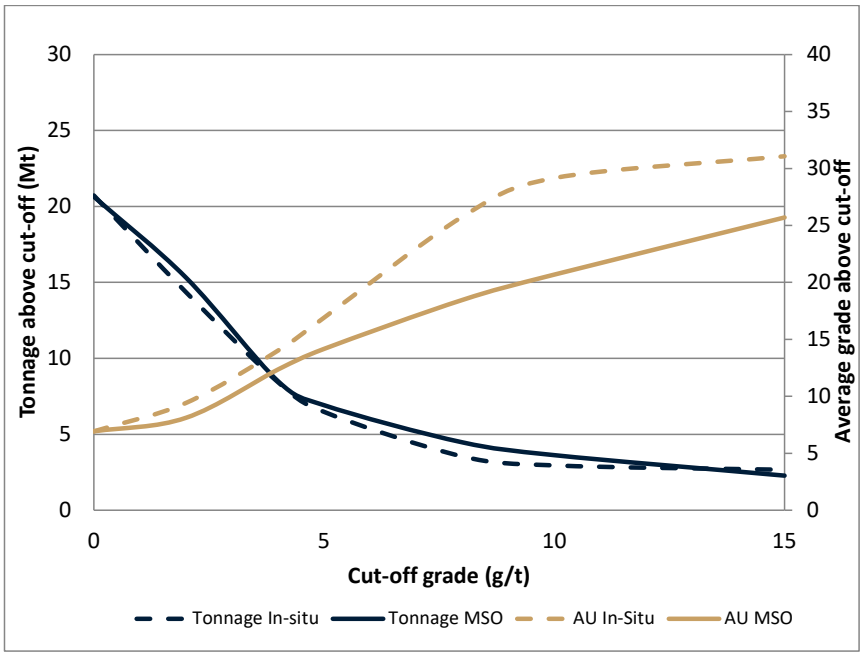

Figure 20. MRC—Grade Tonnage Curve (In Situ vs. MSO Resource).

5. Discussion

The combined use of deterministic and probabilistic methods for modelling vein geology, as proposed by [4], produced satisfactory results at Fairview Mine. The estimated tonnage did not vary significantly from the actual production output. The initial deterministic model provided the large-scale geological trend within which a probabilistic model could be estimated. The iterative nature of probabilistic modelling enabled the analysis of various probable options, facilitating the selection of the model that best captured the underlying geology. This approach allowed for mathematical modelling while incorporating valuable input from geological knowledge and expectations.

Further studies could explore how this approach might be used to optimize future exploration or sampling targets. Additionally, there is potential for enhancing the representation of natural, local-scale variations within ore shoots by incorporating dynamic anisotropy into the AIDW method. To enhance the validation process, it is suggested to incorporate cross-validation along with visual checks and swath plots. Statistical tests could be integrated as part of interpreting swath plot results. Furthermore, the grade interpolation approach could be improved by adopting the domaining guidelines suggested by [64], and by including an assessment of the uncertainty associated with Au grade distribution.

Author Contributions: Conceptualization, methodology, data curation and formal analysis by T.M. and C.J.M.; Investigation, funding and writing by M.I.M., Validation and supervision by H.P. All authors have read and agreed to the published version of the manuscript.

Funding: The APC was funded by the University of the Witwatersrand (School of Mining Engineering).

Data Availability Statement: The data presented in this study are available on request from the corresponding author. The data are not publicly available due to company confidentiality.

Acknowledgments: We would like to extend our sincere appreciation to Pan African Resources PLC for graciously allowing us to use the company's data and resources, which significantly contributed to the success of our research and paper. Their support has been instrumental in advancing knowledge and fostering collaboration between academia and industry. We are truly grateful for the opportunity to cooperate and look forward to potential future collaborations.

Conflicts of Interest: Authors 1 and 2 are employed by Pan African Resources PLC. The remaining authors declare that the research was conducted in the absence of any commercial or financial relationships that could be construed as a potential conflict of interest. The funders had no role in the design of the study; in the collection, analyses, or interpretation of data; in the writing of the manuscript; or in the decision to publish the results.

References

1. Sides, E.J. Geological Modelling of Mineral Deposits for Prediction in Mining. *Geol. Rundsch.* **1997**, *86*, 342–353. [CrossRef]
2. Dominy, S.C.; Platten, I.M.; Raine, M.D. Grade and Geological Continuity in High-Nugget Effect Gold-Quartz Reefs: Implications for Resource Estimation and Reporting. *Trans. Inst. Min. Metall. Sect. B Appl. Earth Sci.* **2003**, *112*, 239–259. [CrossRef]
3. Sterk, R. The Konongo Gold Project, Ghana: An Example of How Geology Makes All the Difference to a Resource Estimate. *Appl. Earth Sci.* **2014**, *112*, 239–259.
4. Rossi, M.E.; Strong, T.J.; Brown, P.J. Geological Modelling of Complex Ore Bodies: Combining Deterministic and Probabilistic Models. In Proceedings of the 5th International Seminar on Geology for the Mining Industry, Santiago, Chile, 23–25 August 2017; GEOMIN: Santiago, Chile, 2017.
5. Ongarbayev, I.; Madani, N. Anisotropic Inverse Distance Weighting Method: An Innovative Technique for Resource Modeling of Vein-Type Deposits. *J. Min. Environ.* **2022**, *13*, 957–972. [CrossRef]
6. Healey, C.M. Geology as a Risk Factor in Project Evaluation: Its Impact on Reserve Estimation. *Explor. Min. Geol.* **1992**, *1*, 243–250.
7. Deutsch, C.V. Mineral Inventory Estimation in Vein Type Gold Deposits: Case Study on the Eastmain Deposit. *CIM Bull.* **1989**, *82*, 62–67.
8. Dominy, S.C.; Annels, A.E. Evaluation of Gold Deposits—Part 1: Review of Mineral Resource Estimation Methodology Applied to Fault- and Fracture-Related Systems. *Trans. Inst. Min. Metall. Sect. B Appl. Earth Sci.* **2001**, *110*, 145–166. [CrossRef]
9. Dominy, S.C.; Simon Camm, G. Resource Evaluation of Narrow Gold-Bearing Veins: Problems and Methods of Grade Estimation. *Trans. Inst. Min. Metall. Sect. A Min. Technol.* **1999**, *1088*, 52–70.
10. Dominy, S.C.; Johansen, G.F.; Cuffley, B.W.; Platten, I.M.; Annels, A.E. Estimation and Reporting of Mineral Resources for Coarse Gold-Bearing Veins. *Explor. Min. Geol.* **2000**, *9*, 13–42. [CrossRef]

11. Dominy, S.C.; Simon Camm, G. Geology in the Resource and Reserve Estimation of Narrow Vein Deposits. *Explor. Min. Geol.* **1997**, *6*, 317–333.
12. Vallée, M. Sampling Quality Control. *Explor. Min. Geol.* **1998**, *7*, 107–116.
13. Dominy, S.C.; Annels, A.E.; Johansen, G.F.; Cuffley, B.W. General Considerations of Sampling and Assaying in a Coarse Gold Environment. *Trans. Inst. Min. Metall. Sect. B Appl. Earth Sci.* **2000**, *109*, 145–167. [CrossRef]
14. Dominy, S.C.; Stephenson, P.R. Classification and Reporting of Mineral Resources for High-Nugget Effect Gold Vein Deposits. *Explor. Min. Geol.* **2001**, *10*, 215–233. [CrossRef]
15. Dominy, S.C. Grab Sampling for Underground Gold Mine Grade Control. *J. South. Afr. Inst. Min. Metall.* **2010**, *110*, 277–287.
16. Dominy, S.; Platten, I.; Glass, H.; Purevgerel, S.; Cuffley, B. Determination of Gold Particle Characteristics for Sampling Protocol Optimisation. *Minerals* **2021**, *11*, 1109. [CrossRef]
17. Dominy, S.; Glass, H.; Purevgerel, S. Sampling for Resource Evaluation and Grade Control in an Underground Gold Operation: A Case of Compromise. *TOS Forum* **2022**, *11*, 375–395. [CrossRef]
18. Dominy, S.C.; Annels, A.E.; Barr, S.P.; Hodkinson, I.P.; Cuffley, B.W. Gold Grade Distribution and Estimation in Narrow Vein Systems. In Proceedings of the PACRIM Congress, Bali, Indonesia, 10–13 October 1999; pp. 411–425.
19. Sims, D. Geological Modelling and Grade Control in a Narrow Vein, High-Grade Gold Mine. In Proceedings of the 4th International Mining Geology Conference, Coolum, Australia, 14–17 May 2000; pp. 65–76.
20. Fowler, A.; Davis, C. Quantifying Uncertainty in a Narrow Vein Deposit—An Example from the Augusta Au-Sb Mine in Central Victoria, Australia. In Proceedings of the 8th International Mining Geology Conference, Queenstown, New Zealand, 22–24 August 2011; pp. 307–318.
21. Charifo, G.; Almeida, J.A.; Ferreira, A. Managing Borehole Samples of Unequal Lengths to Construct a High-Resolution Mining Model of Mineral Grades Zoned by Geological Units. *J. Geochem. Explor.* **2013**, *132*, 209–223. [CrossRef]
22. Daya, A.A. Ordinary Kriging for the Estimation of Vein Type Copper Deposit: A Case Study of the Chelkureh, Iran. *J. Min. Metall.* **2015**, *51*, 1–14. [CrossRef]
23. Vieira Matias, F.; Almeida, J.A.; Chichorro, M. A Multistep Methodology for Building a Stochastic Model of Gold Grades in the Disseminated and Complex Deposit of Casas Novas in Alentejo, Southern Portugal. *Resour. Geol.* **2015**, *65*, 361–374. [CrossRef]
24. Sanches, A.; Almeida, J.; Caetano, P.S.; Vieira, R. A 3D Geological Model of a Vein Deposit Built by Aggregating Morphological and Mineral Grade Data. *Minerals* **2017**, *7*, 234. [CrossRef]
25. Daya, A.A. Nonlinear Disjunctive Kriging for the Estimating and Modeling of a Vein Copper Deposit. *Iran. J. Earth Sci.* **2019**, *11*, 226–236.
26. Dominy, S.C.; Platten, I.M.; Fraser, R.M.; Dahl, O.; Collier, J.B. Grade Control in Underground Gold Vein Operations—The Role of Geological Mapping and Sampling. In Proceedings of the Seventh International Mining Geology Conference, Perth, Australia, 17–19 August 2009; pp. 291–307.
27. Dominy, S.C.; Platten, I.M. Grade Control Geological Mapping in Underground Gold Vein Operations. *Trans. Inst. Min. Metall. Sect. B Appl. Earth Sci.* **2012**, *121*, 96–103. [CrossRef]
28. Knight, R.H. 3D Mine Mapping-Improving Grade Control and Reconciliation in Underground Mines Using Photogrammetric Imagery and Implicit Modelling Techniques. In Proceedings of the Tenth International Mining Geology Conference, Hobart, Tasmania, 20–22 September 2017; The Australasian Institute of Mining and Metallurgy: Melbourne, Australia, 2017; pp. 203–212.
29. Dominy, S.C.; Johansen, G.F. Reducing Grade Uncertainty in High-Nugget Effect Gold Veins-Application of Geological and Geochemical Proxies. In Proceedings of the PACRIM 2004 Congress, Adelaide, Australia, 19–22 September 2004; The Australasian Institute of Mining and Metallurgy: Adelaide, Australia, 2004; pp. 291–302.
30. Dominy, S.C.; Edgar, W.B. Approaches to Reporting Grade Uncertainty in High Nugget Gold Veins. *Trans. Inst. Min. Metall. Sect. B Appl. Earth Sci.* **2012**, *121*, 29–42. [CrossRef]
31. Hill, E.J.; Oliver, N.H.S.; Cleverley, J.S.; Nugus, M.J.; Carswell, J.; Clark, F. Characterisation and 3D Modelling of a Nuggety, Vein-Hosted Gold Ore Body, Sunrise Dam, Western Australia. *J. Struct. Geol.* **2014**, *67*, 222–234. [CrossRef]
32. Mann, C.J. *Computers in Geology—25 Years of Progress*; Davis, J.C., Herzfeld, U.C., Eds.; Oxford University Press: New York, NY, USA, 1993; ISBN 9780195085938.
33. Bárdossy, G.; Fodor, J. Traditional and New Ways to Handle Uncertainty in Geology. *Nat. Resour. Res.* **2001**, *10*, 179–187. [CrossRef]
34. Dominy, S.C.; Annels, A.E.; Noppe, M. Errors and Uncertainty in Ore Reserve Estimates: Operator Beware. In Proceedings of the 8th AusIMM Underground Operators' Conference, Townsville, Australia, 29–31 July 2002; Australasian Institute of Mining and Metallurgy: Townsville, Australia, 2002; pp. 121–126.
35. Dominy, S.C. Errors and Uncertainty in Mineral Resource and Ore Reserve Estimation: The Importance of Getting It Right. *Explor. Min. Geol.* **2002**, *11*, 77–98. [CrossRef]
36. Randle, C.H.; Bond, C.E.; Lark, R.M.; Monaghan, A.A. Uncertainty in Geological Interpretations: Effectiveness of Expert Elicitations. *Geosphere* **2019**, *15*, 108–118. [CrossRef]
37. McManus, S.; Rahman, A.; Coombes, J.; Horta, A. Uncertainty Assessment of Spatial Domain Models in Early Stage Mining Projects—A Review. *Ore Geol. Rev.* **2021**, *133*, 104098. [CrossRef]
38. Dominy, S.C.; Sides, E.J.; Dahl, O.; Platten, I.M. Estimation and Exploitation in an Underground Narrow Vein Gold Operation-Nalunaq Mine, Greenland. In Proceedings of the Sixth International Mining Geology Conference, Darwin, Australia, 21–23

August 2006; Australasian Institute of Mining and Metallurgy Publication Series. Australasian Institute of Mining and Metallurgy: Carlton, Australia, 2006; pp. 29–44.
39. Zhong, D.; Zhang, J.; Wang, L.; Bi, L. Implicit Modeling of Narrow Vein Type Ore Bodies Based on Boolean Combination Constraints. *Sci. Rep.* **2022**, *12*, 6086. [CrossRef] [PubMed]
40. Richmond, A. Conditional Simulation of a Folded Lode-Style Gold Deposit. In Proceedings of the Narrow Vein Mining Conference, Perth, Australia, 26–27 March 2012; The Australasian Institute of Mining and Metallurgy (AusIMM): Carlton, Australia, 2012; pp. 149–154.
41. Machuca-Mory, D.F.; Munroe, M.J.; Deutsch, C.V. Tonnage Uncertainty Assessment of Vein-Type Deposits Using Distance Functions and Location-Dependent Correlograms. In Proceedings of the APCOM2009, Vancouver, BC, Canada, 6–9 October 2009; Volume 11, pp. 115–122.
42. Taylor, I. *Resource Estimate Update of the Wonawinta Silver Project, NSW, Australia*; Spring Hill: Hernando County, FL, USA, 2021.
43. Renard, D.; Wagner, L.; Chilès, J.-P.; Vann, J.; Deraisme, J. Modeling the Geometry of a Mineral Deposit Domain with a Potential Field. In Proceedings of the 36th APCOM Symposium Applications of Computers and Operations Research in the Mineral Industry, Porto Alegre, Brazil, 4–8 November 2013; Fundação Luiz Englert: Porto Alegre, Brazil, 2013.
44. de Carvalho, D.A. *Probabilistic Resource Modeling of Vein Deposits*; University of Alberta: Edmonton, AB, Canada, 2018.
45. Roy, D.; Butt, S.D.; Frempong, P.K. Geostatistical Resource Estimation for the Poura Narrow-Vein Gold Deposit. *CIM Bull.* **2004**, *97*, 47–55.
46. Murphy, M.P.; Ward, C.W. Computer Assisted Modelling of Narrow, Elongate Gold Deposits for Resource Estimation and Mine Planning. In Proceedings of the AuslMM Annual Conference, Ballarat, Australia, 12–15 March 1997; pp. 165–170.
47. Vigar, A.J.; Hills, P.B. Modelling of Multiple Narrow Veins from Geology to Mining—The Tasmania Reef, Beaconsfield, Tasmania. In Proceedings of the PACRIM '99, Bali, Indonesia, 10–13 October 1999; pp. 397–410.
48. Healey, C.M. Performance of Reserve Estimation Techniques in the Presence of Extremely High-Grade Samples, Jasper Gold Mine, Saskatchewan. *Explor. Min. Geol.* **1993**, *2*, 41–47.
49. Manna, B.; Samanta, B.; Chakravarty, D.; Dutta, D.; Chowdhury, A.; Santra, A.; Banerjee, A. Hyperspectral Signature Analysis Using Neural Network for Grade Estimation of Copper Ore. *IOP Conf. Ser. Earth Environ. Sci.* **2018**, *169*, 012108. [CrossRef]
50. Zhang, X.; Song, S.; Li, J.; Wu, C. Robust LS-SVM Regression for Ore Grade Estimation in a Seafloor Hydrothermal Sulphide Deposit. *Acta Oceanol. Sin.* **2013**, *32*, 16–25. [CrossRef]
51. Mutobvu, T.; Cronje, T. *Technical Report on the Modelling and Mineral Resource Estimation of Main Reef Contact (MRC) at Fairview and Sheba Mines, Barberton*; Pan African Resources: Johannesburg, South Africa, 2023.
52. Gloyn-Jones, J.; Kisters, A. Ore-Shoot Formation in the Main Reef Complex of the Fairview Mine—Multiphase Gold Mineralization during Regional Folding, Barberton Greenstone Belt, South Africa. *Miner. Depos.* **2019**, *54*, 1157–1178. [CrossRef]
53. Pan African Resources. *Mineral Resources and Mineral Reserves Report*; Pan African Resources: Johannesburg, South Africa, 2023.
54. Datamine Studio, R.M. Available online: https://docs.dataminesoftware.com/StudioRM/index.htm (accessed on 6 February 2024).
55. Datamine Minimum Curvature Modelling Method—Overview. Available online: https://docs.dataminesoftware.com/StudioRM/Latest/COMMON/Delauney%20Tesselation%20Method%20Overview.htm (accessed on 11 October 2023).
56. Briggs, I.C. Machine Contouring Using Minimum Curvature. *Geophysics* **1974**, *39*, 39–48. [CrossRef]
57. Swain, C.J. A FORTRAN IV Program for Interpolating Irregularly Spaced Data Using the Difference Equations for Minimum Curvature. *Comput. Geosci.* **1976**, *1*, 231–240. [CrossRef]
58. Webring, M. MINC, a Gridding Program Based on Minimum Curvature. USGS Open-File Report 81-1224. Available online: https://pubs.usgs.gov/of/1981/1224/report.pdf (accessed on 11 October 2023).
59. Babak, O. Inverse Distance Interpolation for Facies Modeling. *Stoch. Environ. Res. Risk Assess.* **2014**, *28*, 1373–1382. [CrossRef]
60. Matheron, G. The Theory of Regionalised Variables and Its Application. *Ec. Natl. Super. Mines Paris* **1971**, *5*, 212.
61. Rossi, M.E.; Deutsch, C.V. Recoverable Resources: Estimation. In *Mineral Resource Estimation*; Springer: Dordrecht, The Netherlands, 2014; pp. 133–150.
62. Wilde, B.; Deutsch, C. Programs for Swath Plots. *Cent. Comput. Geostat. Annu. Rep.* **2012**, *14*, 305.
63. Harding, B.; Deutsch, C. Change of Support and the Volume Variance Relation. Geostatistics Lessons 2019. Available online: https://geostatisticslessons.com/lessons/changeofsupport (accessed on 11 October 2023).
64. Sterk, R.; De Jong, K.; Partington, G.; Kerkvliet, S.; Van De Ven, M. Domaining in Mineral Resource Estimation: A Stock-Take of 2019 Common Practice. In Proceedings of the 11th International Mining Geology Conference, Australasian Institute of Mining and Metallurgy, Melbourne, Australia, 25 November 2019; p. 9.